*Proc. Natl. Acad. Sci. USA*
Vol. 90, pp. 9135–9139, October 1993
Biophysics

# Protein hydration elucidated by molecular dynamics simulation

(deviation from x-ray crystal structure/fluctuation/dihedral transitions/glass transition)

PETER J. STEINBACH AND BERNARD R. BROOKS*

Laboratory of Structural Biology, Division of Computer Research and Technology, National Institutes of Health, Bethesda, MD 20892

*Communicated by Martin Karplus, June 3, 1993*

ABSTRACT **Molecular dynamics (MD) simulations covering a wide range of hydration indicate that myoglobin is fully hydrated by 350 water molecules, in agreement with experiment. These waters, originally placed uniformly about the protein, form clusters that hydrate every charged group throughout the entire simulation. Some atoms in charged groups are hydrated by two water layers while 37% of the protein surface remains uncovered. The locations of the 350 waters are consistent with those of crystallographic waters resolved by x-ray and neutron diffraction. Hydration by 350 waters at 300 K stabilizes the conformation of carboxymyoglobin measured by x-ray diffraction throughout the entire protein, halves the rate of torsional transitions, and promotes alternative conformations for surface atoms. The glass transition observed experimentally in hydrated myoglobin near 220 K is also seen in the simulations and correlates with an increase in the number of dihedral angles undergoing transitions. The anharmonic protein motion above 220 K is enhanced by protein hydration.**

Protein hydration has been described as the process of "adding water incrementally to dry protein, until a level of hydration is reached beyond which further addition of water produces no change and only dilutes the protein" (1). The effects of hydration on equilibrium protein structure and dynamics are fundamental to the relationship between structure and biological function and have been extensively studied experimentally (1, 2). Although some dynamic properties show complicated hydration dependences, time-averaged properties can be monitored experimentally to yield well-defined hydration end points. For example, differential scanning calorimetry measurements have suggested that carboxymyoglobin (MbCO) is fully hydrated at 0.39 *h* (g of $H_2O$ per g of protein) (3) or by about 390 waters per protein. Solvation effects have also been explored by molecular dynamics (MD) simulation (4, 5), but no previous simulation study has monitored protein behavior while incrementally changing hydration over a wide range. Upon hydration, increased atomic fluctuation has been observed experimentally for myoglobin (6), but reduced fluctuation has been seen in MD simulations of bovine pancreatic trypsin inhibitor (7). A realistic atomic-level description of the mechanisms by which hydration affects the structure and fluctuation of proteins would further our understanding of protein stability and protein folding and may offer clues to successful protein design.

Expanding upon our study of environmental effects on protein dynamics (8), we report MD simulations of MbCO at 300 K with 14 different hydration levels, from 0 to 3830 waters per protein, and at 100 K with 10 hydration levels. Dehydrated MbCO was simulated at nine temperatures. Structural effects of hydration on the average protein conformation were evident in the best-fit root-mean-square deviation (rmsd) from the structure determined by x-ray diffraction and in the protein's radius of gyration and overall shape. Dynamically, protein hydration was reflected in the simulated torsional transitions and mean-square atomic fluctuation.† The radial distribution functions of the distance separating water oxygen atoms from protein heavy atoms in charged, hydrophilic, and hydrophobic groups were calculated, and the locations of the 350 most essential waters were compared to those of the crystalline water resolved by neutron and x-ray diffraction.

## Computational Methods

All simulations and analysis were performed using the CHARMM program (9). A Polygen (Waltham, MA) all-atom parameter set (10) was used with slight modification to the heme group (11). The TIP3P water model (12) was modified as follows. Hydrogen atoms were given a small van der Waals radius to avoid catastrophically large energies upon the close approach of hydrogen atoms to other atoms. Internal geometry constraints were omitted to provide water flexibility. Unpublished simulations have shown these modifications to yield values for the water density, heat of vaporization, and diffusion coefficient as close to the experimental values as those obtained with the original TIP3P model.

Water molecules taken from a pure water simulation were placed uniformly about the MbCO structure measured by x-ray diffraction (13) based on their distance from the nearest protein atom. The dynamics of the hydrated protein was then simulated in vacuum (8, 11). All simulations were of 150-ps duration using a 1-fs integration time step and a 12-Å shifted potential. Although unrestrained, no more than three waters ever evaporated. Once 12 Å away from all other atoms, evaporated waters no longer interacted with the system and required no special treatment. At each hydration level, 1000 coordinate sets obtained from the final 100 ps of a preliminary 300 K simulation were individually translated and rotated to best fit a reference structure. The oriented coordinate sets were then averaged and energy-minimized to produce the starting structure for subsequent simulations. Only the last 100 ps of these subsequent simulations were analyzed. Dynamics at 300 K was simulated at hydration levels of 0, 35, 50, 60, 80, 100, 125, 150, 225, 350, 600, 1000, 1900, and 3830 waters per protein. The 300-ps protocol was repeated (with different initial velocities) at all hydration levels below 350 waters per protein. Dynamics at 100 K was simulated using the starting structures obtained at 300 K at hydration levels

The publication costs of this article were defrayed in part by page charge payment. This article must therefore be hereby marked "*advertisement*" in accordance with 18 U.S.C. §1734 solely to indicate this fact.

Abbreviations: MD, molecular dynamics; MbCO, carboxymyoglobin.

*To whom reprint requests should be addressed.

†*Radius of gyration* refers to the mass-weighted root-mean-square atomic distance from the center of mass, and *mean-square fluctuation* denotes the mass-weighted variance in position $\langle(\Delta r)^2\rangle$. A *dihedral transition* was considered to occur when the torsion about a single bond moved from one potential well to 30° beyond the barrier to an adjacent well. Correlated dihedral transitions in proline residues were counted as a single transition.

of 0, 35, 60, 100, 150, 225, 350, 600, 1000, and 1900 waters per protein. The dynamics of dehydrated MbCO was also simulated at 50, 150, 175, 200, 225, 250, and 325 K. Simulations were performed on Star Technologies array processors and on an Intel iPSC/860 hypercube, requiring the equivalent of roughly 5000 Cray X/MP hours. The 3830-water system requires 3 Cray X/MP hours per picosecond of simulation. Structural and dynamical effects of hydration were analyzed at the protein surface and in the protein core. An ellipsoid with principal axes proportional to those of the protein was used to classify half of the 2536 protein atoms as inner atoms and half as outer atoms.

The overall shapes of structures were quantified by the anisotropies $A_1$ and $A_2$:

$$A_l = \left( \frac{2\sum m_i x_{li}^2}{\sum m_i x_{2i}^2 + \sum m_i x_{3i}^2} \right)^{1/2} - 1.0. \qquad [1]$$

Here, the $x_1$ axis is the major axis of the structure and the $x_2$ axis specifies the direction of greatest extent perpendicular to the $x_1$ axis. $A_1$ and $A_2$ are thus measures of deviation from spherical and from cylindrical symmetry, respectively.

Accessible surface areas were calculated (14) after assigning atomic radii to all non-hydrogen atoms (15). To characterize only the exterior protein surface, interior cavities were first filled with dummy atoms, thus avoiding contributions from the heme pocket and other interior surfaces. The probe radius was 1.4 Å. Protein heavy atoms were classified as charged (the N and C termini and the end groups of Asp, Glu, Arg, and Lys, and the heme's proprionic acid side chains; 121 in all), uncharged hydrophilic (all other carbon atoms with charge >0.31 e and all other oxygen and nitrogen atoms; 546 in all), and hydrophobic (the remaining 595 heavy atoms).

### Protein Structure and Dynamics

The rmsd of the time-averaged protein structure from the x-ray structure quantitatively characterizes the global conformation of the simulated molecule. On the 100-ps time scale, the crystalline conformation of MbCO (13) was stabilized by 350 water molecules, and no significant change occurred upon further hydration (Fig. 1*A*). MbCO hydrated by 100 or fewer water molecules deviated from the crystal structure by an average of 1.0 ± 0.1 Å rms more than MbCO hydrated by 350 or more waters. This 1.0-Å increase in rmsd was seen for inner and outer atoms, demonstrating that the entire protein underwent a pronounced conformational deformation when inadequately hydrated.

Fig. 1 *B* and *C* show the size and shape of the simulated structures, respectively. The radii of gyration of the backbone and of the entire protein were similar at 300 K and increased with hydration, approaching those of the crystalline conformation at hydration above 1000 waters per protein (Fig. 1*B*). The similarity in backbone and protein radii indicates that the protein swelling with hydration was not primarily due to the extension of surface side chains upon solvation. Because of surface tension acting on the hydrated protein, simulation at every hydration level produced a protein structure more spherical (characterized by a smaller $A_1$ value) than the crystal structure (Fig. 1*C*). The pressure within the protein due to surface tension is expected to decrease with increased hydration. The protein shape was hydration independent (Fig. 1*C*), suggesting that the protein swelling with hydration was a global and homogeneous response to this reduced pressure. The increase in free volume associated with the protein swelling at hydration above 100 waters per protein may enhance mobility by facilitating collective motions. Upon cooling to 100 K, the radius of gyration decreased by about 1%, consistent with the

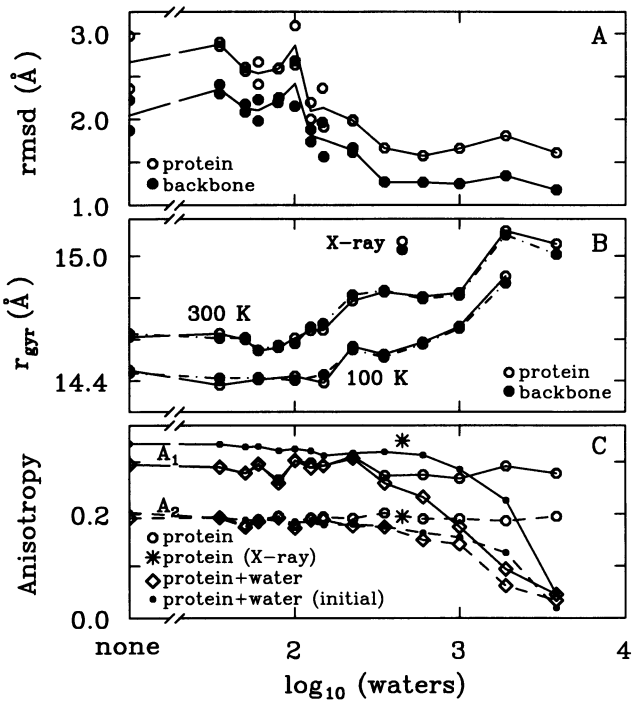


FIG. 1. (*A*) Mass-weighted rmsd of the time-averaged 300 K structure from the x-ray structure (13) vs. the number of associated water molecules, determined for the 459 backbone (N, C, and $C_\alpha$) atoms and for all 2536 MbCO atoms. Lines depict averages over two simulations at hydration below 350 waters per protein. (*B*) Radii of gyration of the average backbone and protein structures at 100 and 300 K. (*C*) Anisotropy of shape at 300 K of the average protein and protein/water structures and of the initial protein/water configuration. $A_1$ and $A_2$ are plotted as solid and dashed lines, respectively. For clarity in *B* and *C*, only average results are plotted at hydration below 350 waters per protein. The radii of gyration and structural anisotropies of the crystalline conformation (260 K) are plotted at 450 waters per protein, a hydration level estimated from the unit cell volume.

3% decrease in volume of the unit cell of metmyoglobin crystals from 300 to 80 K (16).

Fig. 1*C* also shows that surface tension did not significantly alter the configuration of the water molecules until hydration exceeded 350 waters per protein. Because each hydration level was initially achieved by selecting from a sphere of water molecules all waters within a given distance of any protein atom, the initial protein–water structure possessed the shape of the protein at low hydration and the shape of the sphere of water ($A_1 \approx A_2 \approx 0$) at a hydration of 3830 waters per protein. During simulation, protein–water interactions competed with surface tension to determine the shape of the average protein–water system. Only at hydration above 350 waters per protein did the average structure of the protein–water system become considerably more spherical than the protein. Thus, protein–water interactions appear to have dominated surface tension effects at hydration at and below 350 waters per protein.

Because protein motion enables protein function, the influence of hydration on protein dynamics is of particular interest. Solvent can slow protein motions by introducing friction, and it can alter motional amplitudes by changing the equilibrium structure of the protein (17). The slowing of protein motion is evident in Fig. 2*A*, which shows that the number of heavy-atom dihedral transitions (filled circles) observed at 300 K was halved upon increasing hydration from 0 to 350 waters per protein but was not significantly reduced upon further hydration. By contrast, the number of dihedral angles undergoing transitions (open circles, times 5) changed

little with hydration. The mean-square fluctuation, $\langle(\Delta r)^2\rangle$, of interior protein atoms was not greatly affected by hydration at 300 K (Fig. 2*B*). However, the fluctuation of the outermost protein atoms was increased significantly; the hydration water served as a "mobility catalyzer" (18). There was an appreciable correlation at 300 K between the hydration dependences of the number of dihedral angles undergoing one or more transitions (Fig. 2*A*, open circles) and the protein fluctuation $\langle(\Delta r)^2\rangle$ (Fig. 2*B*, open circles). As discussed below, a correlation was also observed between the *temperature* dependences of the number of dihedral angles undergoing transitions and the anharmonic contribution to $\langle(\Delta r)^2\rangle$. These two correlations indicate that at high temperatures torsional motion accounts for much of the protein's conformational exploration.

Although surface fluctuation was enhanced by hydration at 300 K, it was approximately halved by the accumulation of an "icy" solvent at 100 K. The number of dihedral angles undergoing transitions at 100 K decreased from only six at hydration by 0 and 35 waters per protein to zero at hydration by 1900 waters per protein.

Although one observable, myoglobin's radius of gyration, continued to change, our simulations indicate that hydration of MbCO beyond 350 waters per protein produces no significant changes in protein behavior on the 100-ps time scale and essentially "only dilutes the protein." We now examine the effects of these 350 hydration waters in greater detail.

### Glass Transition

Fig. 3*A* shows the temperature dependence of $\langle(\Delta r)^2\rangle$ for hydrated and for dehydrated MbCO. Our simulations of hydrated MbCO at multiple temperatures (11) agree remarkably well with neutron scattering experiments performed on myoglobin powders (19) with regard to the glass-transition temperature, about 220 K, and the anharmonic fluctuation occurring at higher temperatures (Fig. 3*B*). This transition to anharmonicity, seen in many proteins, can be essential for function. For example, following flash photolysis, myoglobin rebinds CO or $O_2$ appreciably from the solvent only at temperatures above the transition (20). Similarly, crystalline ribonuclease A binds either substrate or inhibitor rapidly above the transition but not below (21). Compared to experiment, our previous simulations (8) have overestimated the harmonic fluctuation of hydrated MbCO (19, 22) and our current simulations have overestimated the harmonic fluctuation of dehydrated MbCO (6). However, our simulations do agree with experiment by revealing a significant increase in anharmonic fluctuation above the glass-transition temperature upon hydration (Fig. 3*B*). Increasing the temperature and hydration leads to a more flexible protein. Given that myoglobin fluctuation increases upon hydration, as observed experimentally and theoretically, the reduced fluctuation of bovine pancreatic trypsin inhibitor upon solvation at 310 K seen in MD simulations (7) is difficult to interpret.

For hydrated and for dehydrated MbCO, the number of dihedral angles undergoing transitions as a function of temperature was scaled to the anharmonic fluctuation, $\langle(\Delta r)^2\rangle_{anh}$. At both hydration levels, the temperature dependence of the number of dihedral angles undergoing transitions was nearly identical to that of the anharmonic motion (Fig. 3*B*). Since the anharmonic motion simulated for hydrated myoglobin agrees quantitatively with that measured by neutron scattering (11), our results strongly suggest that the interconversion of torsional substates contributes significantly to the glass transition in myoglobin near 220 K and that the torsional barriers used in the simulation are quite realistic. About two-thirds of the dihedral angles undergoing transitions were in the outer half of the protein. Nonetheless, the number of dihedral angles undergoing transitions increased abruptly near 220 K in the inner and outer protein regions; the simulated glass transition was global (11). The thermal activation of torsional motion near 220 K is presumably common to all globular proteins and is likely fundamental to the similar, functionally relevant transitions observed in many proteins (19, 21, 23, 24).

The constant needed to scale the number of dihedral angles undergoing transitions to $\langle(\Delta r)^2\rangle_{anh}$ was about twice as large for hydrated MbCO as it was for dehydrated MbCO, suggesting that either hydration increases the effect that torsional interconversion has on $\langle(\Delta r)^2\rangle_{anh}$ or it enhances anharmonicity through more global, collective motions (25).

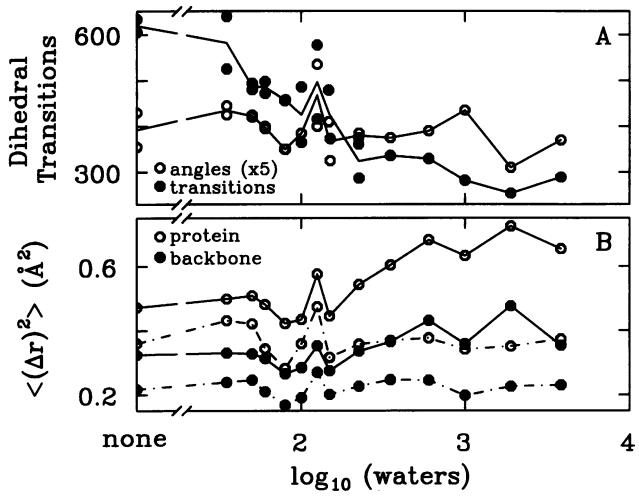


FIG. 2. (*A*) Number of heavy-atom (without hydrogen) dihedral transitions observed and the number of heavy-atom dihedral angles undergoing transitions (times 5) during 100 ps at 300 K. Lines depict averages over two simulations at hydration below 350 waters per protein. (*B*) Mean-square fluctuation $\langle(\Delta r)^2\rangle$ at 300 K for the backbone and protein atoms. Values for inner and outer atoms are plotted as dot-dashed and solid lines, respectively. For clarity, only average results are plotted at hydration below 350 waters per protein.

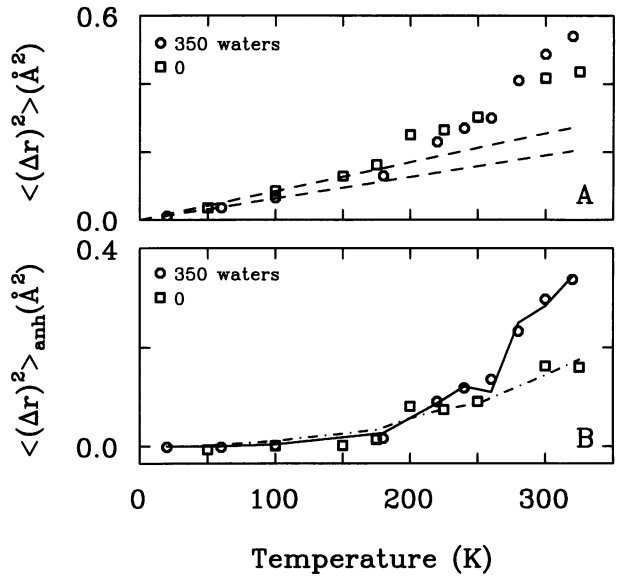


FIG. 3. (*A*) Mean-square fluctuation $\langle(\Delta r)^2\rangle$, averaged over all protein atoms for simulations of MbCO hydrated by 0 and by 350 water molecules (11). Harmonic fluctuation is extrapolated to high temperature (dashed lines). (*B*) Anharmonic contribution to $\langle(\Delta r)^2\rangle$ obtained upon subtraction of the extrapolated harmonic contribution. The lines represent the number of dihedral angles undergoing transitions, scaled independently for the two hydration levels.

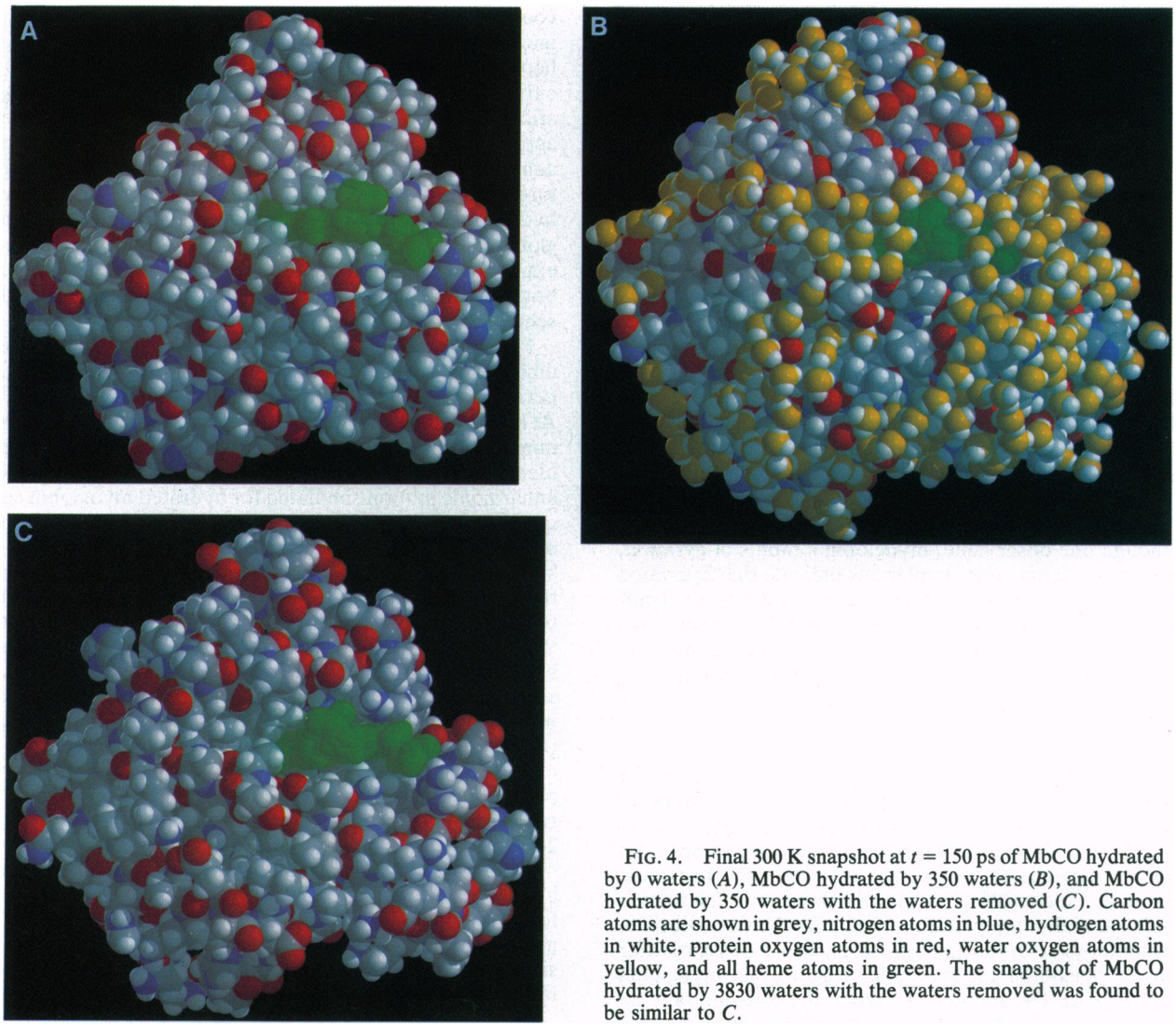


FIG. 4. Final 300 K snapshot at $t = 150$ ps of MbCO hydrated by 0 waters (*A*), MbCO hydrated by 350 waters (*B*), and MbCO hydrated by 350 waters with the waters removed (*C*). Carbon atoms are shown in grey, nitrogen atoms in blue, hydrogen atoms in white, protein oxygen atoms in red, water oxygen atoms in yellow, and all heme atoms in green. The snapshot of MbCO hydrated by 3830 waters with the waters removed was found to be similar to *C*.

For example, without increasing the number of dihedral angles undergoing transitions, hydration could increase $\langle(\Delta r)^2\rangle_{anh}$ by stabilizing the lesser populated dihedral conformations for one or more crucial dihedral angles. Averaged over all dihedral angles, the times spent in the second and third most populated wells were in fact not affected much by hydration. Therefore, collective motions not requiring dihedral transitions may well be responsible for about half of hydrated myoglobin's $\langle(\Delta r)^2\rangle_{anh}$.

### Hydration Waters

To characterize the simulated "hydration shell" of 350 waters, the accessible surface area was calculated for the final configurations of MbCO hydrated by 0 and by 350 waters. The charged surface area increased from 13% of the protein surface for dehydrated MbCO to 25% for hydrated MbCO. The surface was 18% uncharged hydrophilic in both cases, while the fractional hydrophobic area decreased from 69% in vacuum to 57% with 350 waters. Thus, the conformational change observed upon hydration (Fig. 1*A*) exposed charged atoms to solvent and buried hydrophobic atoms. These conformational differences are subtle but evident in Fig. 4 *A* and *C*. The hydrated protein surface (Fig. 4*C*) appears more rugged and shows an increased exposure of oxygen atoms (e.g., near the top of Fig. 4*C*). The 350 hydration waters covered 83% of the charged surface, 65% of the hydrophilic surface, and 53% of the hydrophobic surface, leaving 37% of the protein surface uncovered (Fig. 4*B*).

While the hydration waters exerted forces on the protein, stabilizing its structure and facilitating the motion of its surface atoms, the protein exerted forces on the water, imposing order on it. This order is clearly seen in the radial distribution function, $g_{charged}(r)$, of the distance between MbCO's heavy atoms in charged groups and the waters' oxygen atoms (Fig. 5*A*). The $g(r)$ distributions were similarly computed for MbCO's heavy hydrophilic and hydrophobic atoms (Fig. 5*B*). These distributions give the number of water oxygen atoms, $n(r)$, observed in the simulation at a distance between $r - \delta$ and $r + \delta$ from any protein atom of a specific class, averaged over the $N_a$ protein atoms of the given class and over the $N_c$ coordinate sets analyzed, and normalized by the average number density of water, $\rho = 0.033$ Å$^{-3}$.

$$g(r) = \frac{\frac{1}{N_a N_c}\sum_{i=1}^{N_a}\sum_{j=1}^{N_c} n_{i,j}(r)}{\frac{4\pi\rho}{3}\left((r+\delta)^3 - (r-\delta)^3\right)}. \qquad [2]$$

Two peaks, centered near 3 and 5 Å, were resolved in $g_{charged}(r)$ even at hydration as low as 350 waters per protein, in agreement with neutron diffraction analysis of hydration in MbCO crystals (26). It was apparently energetically prefer-

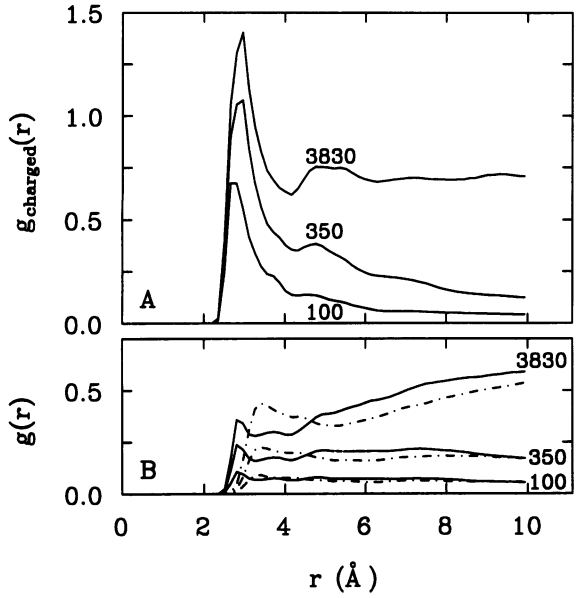


FIG. 5. Radial distribution functions of the distance separating water-oxygen atoms and the protein's charged heavy atoms (*A*) and hydrophilic (solid) and hydrophobic (dot-dash) heavy atoms (*B*). Results are shown for hydration levels of 100, 350, and 3830 waters per protein. The distributions do not approach unity at long distance because of the excluded protein volume and the limited amount of water present.

able for the 350-water simulation to hydrate some atoms in charged groups by two water layers than to more uniformly cover myoglobin with water (Fig. 4*B*). The second peak is not very pronounced even at 3830 waters per protein, indicating that the ordering of the water by the protein was of short range.

The simulated hydration shell of 350 waters compares well with those resolved in two crystallographic studies of MbCO. The first hydration layer about atoms in charged groups (Fig. 5*A*) suggests that a protein heavy atom is hydrated if a water oxygen is within 4 Å. According to this definition, 303 heavy atoms were hydrated by the 89 waters resolved by neutron diffraction (26) and 418 were hydrated by the 137 waters resolved by x-ray diffraction (13). Of the 303 (418) protein heavy atoms hydrated in the neutron (x-ray) structure, 200 (278) were hydrated during 95% or more of the 350-water simulation, 267 (380) were hydrated at least 50% of the time, and only 6 (5) were never hydrated.

Given the 4-Å criterion for hydration, 118 of the 121 heavy atoms in charged groups were always hydrated during the 350-water simulation, and the other 3 were hydrated at least 93% of the time. By contrast, the two 100-water simulations left 6 ± 1 charged atoms unhydrated >10% of the time and each left one charged atom unhydrated >88% of the time. This suggests that the number and arrangement of charged groups on the surface of globular proteins largely determine the number of waters needed for full hydration.

## Conclusions

This study serves as a guide to the realistic simulation of globular proteins on the 100-ps time scale by identifying the significant effects of protein hydration while demonstrating that only a moderate number of water molecules is critically needed, primarily to hydrate charged surface groups. The extensive set of simulations reported here indicates that myoglobin is fully hydrated by 350 water molecules, or 0.35 *h*, in agreement with experimental hydration estimates obtained calorimetrically for myoglobin (0.39 *h*) (3) and for lysozyme (0.38 *h*) (27). The hydration shell of 350 water molecules is not a uniform monolayer but a patchwork of water clusters, covering some atoms in charged groups by two water layers while leaving 37% of the protein surface uncovered. Structurally, all myoglobin atoms feel the stabilizing effect of these water molecules. Dynamically, hydration halves the number of heavy-atom dihedral transitions while permitting greater mobility for surface atoms and promoting the glass transition to anharmonicity that enables myoglobin to function.

We thank W. A. Eaton, M. Levitt, R. W. Pastor, V. A. Parsegian, and D. C. Chatfield for suggestions and the Computing Science and Engineering Section of the Division of Computer Research and Technology (National Institutes of Health) for support on the Intel iPSC/860 hypercube. P.J.S. thanks the National Research Council for a postdoctoral research associateship.

1. Rupley, J. A. & Careri, G. (1991) *Adv. Prot. Chem.* **41**, 37–172.
2. Colombo, M. F., Rau, D. C. & Parsegian, V. A. (1992) *Science* **256**, 655–659.
3. Doster, W., Bachleitner, A., Dunau, R., Hiebl, M. & Lüscher, E. (1986) *Biophys. J.* **50**, 213–219.
4. Brooks, C. L., III, Karplus, M. & Pettitt, B. M. (1988) in *Proteins: A Theoretical Perspective of Dynamics, Structure, and Thermodynamics*, eds. Prigogine, I. & Rice, S. A. (Wiley, New York), pp. 137–174.
5. Lautz, J., Kessler, H., van Gunsteren, W. F., Weber, H.-P. & Wenger, R. M. (1990) *Biopolymers* **29**, 1669–1687.
6. Krupyanskii, Y. F., Parak, F., Goldanskii, V. I., Mössbauer, R. L., Gaubman, E. E., Engelmann, H. & Suzdalev, I. P. (1982) *Z. Naturforsch. C* **37C**, 57–62.
7. Levitt, M. & Sharon, R. (1988) *Proc. Natl. Acad. Sci. USA* **85**, 7557–7561.
8. Steinbach, P. J., Loncharich, R. J. & Brooks, B. R. (1991) *Chem. Phys.* **158**, 383–394.
9. Brooks, B. R., Bruccoleri, R. E., Olafson, B. D., States, D. J., Swaminathan, S. & Karplus, M. (1983) *J. Comp. Chem.* **4**, 187–217.
10. Polygen Corp. (1986) Parameter file for CHARMM (Polygen Corp., Waltham, MA), Version 20.
11. Loncharich, R. J. & Brooks, B. R. (1990) *J. Mol. Biol.* **215**, 439–455.
12. Jorgensen, W. L., Chandrasekhar, J., Madura, J. D., Impey, R. W. & Klein, M. L. (1983) *J. Chem. Phys.* **79**, 926–935.
13. Kuriyan, J., Wilz, S., Karplus, M. & Petsko, G. A. (1986) *J. Mol. Biol.* **192**, 133–154.
14. Lee, B. & Richards, F. M. (1971) *J. Mol. Biol.* **55**, 379–400.
15. Shrake, A. & Rupley, J. A. (1973) *J. Mol. Biol.* **79**, 351–371.
16. Frauenfelder, H., Hartmann, H., Karplus, M., Kuntz, I. D., Jr., Kuriyan, J., Parak, F., Petsko, G. A., Ringe, D., Tilton, R. F., Jr., Connolly, M. L. & Max, N. (1987) *Biochemistry* **26**, 254–261.
17. van Gunsteren, W. F. & Karplus, M. (1982) *Biochemistry* **21**, 2259–2274.
18. Chirgadze, Y. N. & Ovsepyan, A. M. (1972) *Biopolymers* **11**, 2179–2186.
19. Doster, W., Cusack, S. & Petry, W. (1989) *Nature (London)* **337**, 754–756.
20. Austin, R. H., Beeson, K. W., Eisenstein, L., Frauenfelder, H. & Gunsalas, I. C. (1975) *Biochemistry* **14**, 5355–5373.
21. Rasmussen, B. F., Stock, A. M., Ringe, D. & Petsko, G. A. (1992) *Nature (London)* **357**, 423–424.
22. Nienhaus, G. U., Heinzl, J., Huenges, E. & Parak, F. (1989) *Nature (London)* **338**, 665–666.
23. Morozov, V. N. & Gevorkian, S. G. (1985) *Biopolymers* **24**, 1785–1799.
24. Nocek, J. M., Stemp, E. D. A., Finnegan, M. G., Koshy, T. I., Johnson, M. K., Margoliash, E., Mauk, A. G., Smith, M. & Hoffman, B. M. (1991) *J. Am. Chem. Soc.* **113**, 6822–6831.
25. Nienhaus, G. U., Hartmann, H., Parak, F., Heinzl, J. & Huenges, E. (1989) *Hyperfine Interactions* **47**, 299–310.
26. Cheng, X. & Schoenborn, B. P. (1990) *Acta Cryst. B* **46**, 195–208.
27. Yang, P. & Rupley, J. A. (1979) *Biochemistry* **18**, 2654–2661.